

Peak effect of critical current densities of $\text{Bi}_2\text{Sr}_2\text{CaCu}_2\text{O}_{8+\delta}$ superconducting whiskers at high temperatures in a low-field regime

著者別名	池田 博
journal or publication title	Physical review B
volume	74
number	6
page range	064514
year	2006-08
権利	(C)2006 The American Physical Society
URL	http://hdl.handle.net/2241/104025

doi: 10.1103/PhysRevB.74.064514

Peak effect of critical current densities of $\text{Bi}_2\text{Sr}_2\text{CaCu}_2\text{O}_{8+\delta}$ superconducting whiskers at high temperatures in a low-field regime

M. Tange,¹ H. Ikeda,^{1,2} and R. Yoshizaki^{1,2}¹*Faculty of Frontier Science, Graduate School of Pure and Applied Sciences, University of Tsukuba, Tsukuba, Ibaraki 305-8571, Japan*²*Cryogenics Division, Research Facility Center for Science and Technology, University of Tsukuba, Tsukuba, Ibaraki 305-8577, Japan*

(Received 22 May 2006; revised manuscript received 28 July 2006; published 30 August 2006)

For $\text{Bi}_2\text{Sr}_2\text{CaCu}_2\text{O}_{8+\delta}$ (Bi-2212) high- T_c superconducting whiskers, we investigate the dependence of critical current densities J_c on magnetic fields along the crystal c axis at elevated temperatures around 70 K by electrical transport measurements, where a dc current is applied along the longest dimension, i.e., the a axis, of the whisker. The voltage-current (V - I) characteristics are varied nonmonotonically by the applied magnetic field H . It is found that J_c increases with the field in the low-field regime near the lower critical field H_{c1} and then decreases with increasing field. The peak of $J_c(H)$ occurs below several tens of oersteds, which is remarkably low by comparison with the conventional peak effect in Bi-2212 bulk single crystals. In addition to the enhancement of J_c , the field-induced zero-voltage state is confirmed to be a function of the magnetic field. The present peak effect is a phenomenon involving dilute vortices confined by surface barriers in a finite narrow width, which is of the order of the translational correlation length with respect to the triangular vortex lattice. The low-field-induced peak effect for a quasi-one-dimensional geometry with surface barriers is discussed.

DOI: [10.1103/PhysRevB.74.064514](https://doi.org/10.1103/PhysRevB.74.064514)

PACS number(s): 74.25.Sv, 74.25.Qt, 74.72.Hs

I. INTRODUCTION

In type-II superconductors, the vortex state under low magnetic fields near the lower critical field H_{c1} is governed by the elasticity of vortices, thermal fluctuations, and the dimensional contribution of the superconducting anisotropy to the fluctuations rather than the bulk pinning due to crystal defects. The characterization of dilute vortices is useful for understanding the correlation of vortices. In an actual system, surface barriers such as Bean-Livingston surface barriers¹ (BLSBs) and geometrical barriers^{2,3} (GBs) are induced owing to the surface or edge of the samples. Consequently, it is necessary to take the effect of the surface barriers into account for the characterization of dilute vortices. The energy potential induced by the surface barriers causes the suppression of thermal vortex depinning, i.e., the magnetic flux penetrating a sample is pushed toward the center of the sample by the Lorentz force due to the Meissner screening current. As a result, the surface barriers produce remarkably different vortex dynamics with regard to the behavior described on the basis of the Bean model:⁴ a vortex dome induced by GBs,³ the suppression of the vortex motion that appears as a sharp drop in the electrical resistance in the vicinity of the bulk first-order melting transition,⁵ and an asymmetric shape between the ascending and descending branches of the magnetization loop.⁶ In particular, for microscopic platelet samples, the surface barriers make the properties of the dilute vortices complicated because the ratio of the surface region, i.e., the flux-free region,⁷ to the sample volume is large by comparison with that of bulk samples.

The properties of dilute vortices have been investigated to obtain knowledge of the vortex dynamics at a finite size. For two-dimensional geometry with a finite sample thickness in low- T_c and high- T_c bulk superconductors, dilute vortices have been visualized and characterized by magneto-optical

techniques,⁸⁻¹⁰ the Bitter decoration method,^{11,12} and the Hall-probe array technique.³ However, for a quasi-one-dimensional geometry as in whiskers, where the influence of the surface and edge is more dominant with regard to the properties of the dilute vortices than in the case of bulk samples, the vortex dynamics influenced by the surface barriers is not well understood because of difficulties in sample preparation and the limitation of the experimental techniques.

The magnetic flux that penetrates a platelet sample varies according to the aspect ratio (width-to-thickness ratio) of the sample because of the BLSBs and GBs, although the dependence of the penetration field H_p for the BLSBs on the aspect ratio is not due to the existence of the surface barrier but to the demagnetization factor.^{3,13-16} In fact, vortex motion is influenced intensely by the BLSBs and the flux penetration is suppressed in a wide range of temperatures, as reported for $\text{Bi}_2\text{Sr}_2\text{CaCu}_2\text{O}_{8+\delta}$ (Bi-2212) high- T_c superconducting whiskers in Refs. 17 and 18. Moreover, at high temperatures, GBs rather than BLSBs dominate the flux penetration owing to flux creep, as described for a platelet sample.¹⁹ The contribution of GBs is characterized as hysteretic behavior in the magnetization loops observed at high temperatures where bulk pinning is almost ineffective. The magnitude of the hysteresis varies according to the shape of the sample; in particular, for platelet samples, the vortex motion is influenced significantly.^{20,21}

For the investigation of superconducting properties influenced by such surface barriers in small samples, Bi-2212 whiskers have a favorable morphology: a high crystallinity that leads to a regular geometry. The whiskers are striplike crystals with tiny cross sections on a micrometer or submicrometer scale. It is known that the a , b , and c crystal axes of the as-grown whisker are parallel to the directions of the length, width, and thickness, respectively. With regard to the

properties of Bi-2212 whiskers with tiny cross sections, although the magnetic properties under magnetic fields along the c axis have been reported using the Hall-probe array technique,^{17,18} the dynamic properties of the dilute vortices remain indistinct because very few studies have reported using dynamic measurements like electrical transport measurement under low magnetic fields. In high- T_c superconducting whiskers, the critical current density J_c , which reflects the pinning force of vortices, is expected to exhibit a complicated dependence on the magnetic field owing to the surface barriers and the small sample size. Revealing the behavior of J_c with respect to the field in Bi-2212 whiskers is important for applications of high- T_c superconducting whiskers to actual devices with transport current as well as for gaining insight into the fundamental physics of vortices in small crystals.

In the present paper, J_c in Bi-2212 whiskers with narrow widths is measured as a function of the magnetic field along the crystal c axis by electrical transport measurements. As a result, the peak effect of J_c is observed in the low-field regime and the enhancement in J_c is verified by a field-induced zero-voltage state. In addition, the peak effect is discussed to clarify the influence of the finite size, i.e., the narrow widths of samples, and the surface barriers on dilute vortices.

II. EXPERIMENT

The Bi-2212 whiskers were prepared under the following conditions by a simple fabrication method, namely, the self-powder-compaction method.²² The growth temperature, oxygen partial pressure in the growth atmosphere, and growth time were 875 °C, 0.2 atm, and 100 h, respectively. A mixture of O₂ and Ar gases flowed during the heat treatment for the control of the oxygen partial pressure. In this work, Bi_{2+x}Sr_{2-x}CaCu₂O_{8+δ} ($x=0.2$) was chosen for the composition of the pellets used as the precursor for the growth of the Bi-2212 whiskers. Whiskers with narrow widths below approximately 10 μm were used for the electrical transport measurements because the surface barriers are sensitive to crystallinity, similar to their sensitivity to the surface condition. In the present paper, among several measured whiskers, data are presented for two samples A and B with different widths. The length, width, and thickness of sample A were 680, 7.1, and 0.8 μm and those of sample B were 508, 5.4, and 0.6 μm, respectively. The thickness-to-width ratio t/w for sample A was approximately equal to that of sample B, which was approximately 0.11. A standard four-probe technique was employed with silver-coated electrical contacts for the electrical transport measurements on the individual Bi-2212 whiskers. A dc current was applied along the a axis. The temperature dependence of the electrical resistivity was investigated using a transport current of 10 μA, which corresponded to the current density ranging from 100 to 400 A/cm². The assumption that the nonlinear effect due to the current density was negligibly small was confirmed by the Ohmic behavior of the voltage measured at 200 K. Voltage-current (V - I) characteristics were measured at high temperatures in the range 70–77 K below T_c in the absence and presence of applied magnetic fields along the c

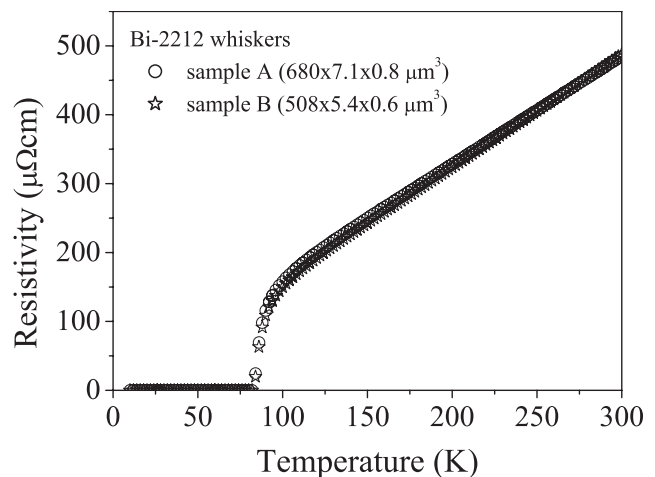


FIG. 1. Temperature dependence of the electrical resistivity measured by passing a transport current along the a axis of samples A and B.

axis. J_c in the direction of the a axis was estimated from the V - I curves. The voltage value of 0.5 μV was used to determine the values of J_c . Electric fields corresponding to this voltage were 26 μV/cm for sample A and 18 μV/cm for sample B. In addition to the measurement of the V - I characteristics, the voltage was measured for a fixed transport current and a constant temperature in the same temperature range with magnetic field ramping. The field along the c axis was ramped up or down to individual target fields at 5 Oe intervals step by step with a waiting time of 3 s. The ramping time from one target field to the next was approximately 60 s. The electrical transport measurement was carried out using a physical property measurement system (PPMS; Quantum Design), a commercial dc current source, and a commercial nanovoltmeter.

III. RESULTS AND DISCUSSION

Figure 1 shows the electrical resistivity ρ as a function of the temperature for samples A and B. The samples are almost identical with regard to the temperature dependence of their resistivities. In addition, the samples have a single-step superconducting transition with $T_{c,zero}=82$ K, which is defined as the temperature where the resistivity falls by four orders of magnitude compared to the value at 300 K. These results suggest that the carrier densities of the samples are almost identical. The whiskers are estimated to be slightly overdoped.²³ With regard to the flux penetration, the thickness-to-width ratios t/w of the samples with rectangular cross sections are an important factor for taking into account the influence of the surface barriers. As the ratio becomes larger, the penetration of flux into the sample is suppressed, namely, H_p becomes higher.^{3,13–16} Therefore, it is considered that the magnitude of H_p for sample A is similar to that for sample B because the samples have the same value of the ratio; the difference in the longest dimension between samples A and B may result in a slight discrepancy in the behavior of the flux penetration.

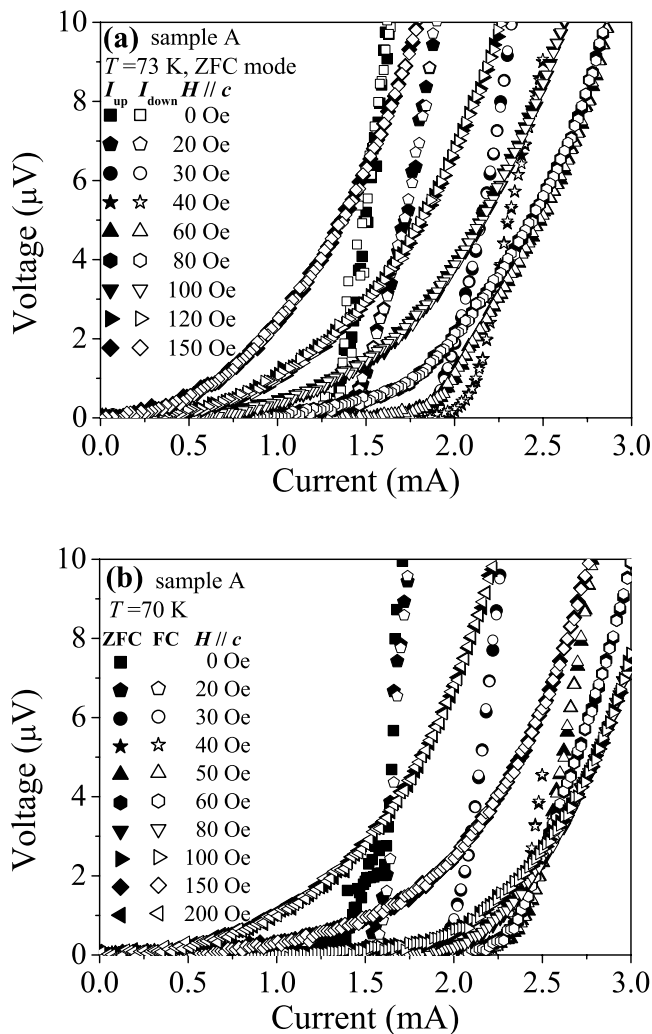


FIG. 2. V - I characteristics with the configuration of $I \parallel a$ axis and $H \parallel c$ axis for sample A. (a) V - I curves for increasing (closed symbols) and decreasing (open symbols) current at 73 K for the ZFC mode. (b) V - I curves at 70 K for the ZFC (closed symbols) and FC (open symbols) modes.

Figure 2(a) shows the V - I curves obtained for sample A at 73 K under various magnetic fields for the zero-field-cooled (ZFC) mode; this means that the field was applied after the zero-field cooling of the sample. The V - I curves for the increasing current are almost the same as those for the decreasing current. This reversibility between the increasing and decreasing processes is also obtained in the case of the V - I curves for the field-cooled (FC) mode, which implies the measurement after field cooling to 70 K. The absence of hysteresis in the V - I curves suggests that the influence of edge contamination, which was observed by Paltiel *et al.* in the case of a strip configuration in Ref. 24, on the state of the vortices that penetrate to the center of the sample is negligible. If the edge contamination acted prominently on the vortex state for the increasing process, a metastable disordered vortex state would be created in the bulk region. Moreover, in this context, the critical current would become lower for the decreasing process because of the annihilation of the disordered vortex state; this was shown in the presence of a dc driving current by Paltiel *et al.*²⁵ Normally, such a phe-

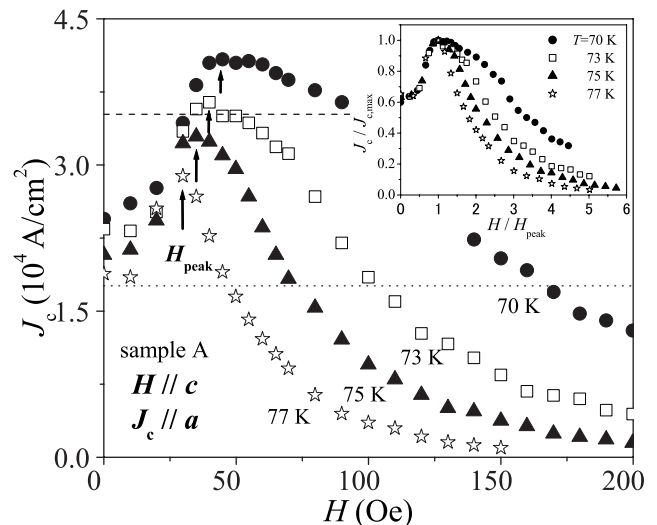


FIG. 3. Field dependence of J_c as estimated from V - I curves at high temperatures in the range of 70 to 77 K for sample A. H_{peak} for 77, 75, 73, and 70 K is approximately 30, 35, 40, and 45 Oe, respectively. The normalized dependence of critical current densities on magnetic fields is plotted in the inset, where the fields and the critical current densities are normalized by the magnitude of H_{peak} and maximum value of J_c , respectively. In the main panel, the current density level represented by the dotted line corresponds to 1.0 mA of the transport current, whereas that for the dashed line corresponds to 2.0 mA.

nomenon due to the edge contamination is observed under weak thermal fluctuations in materials with surface barriers, e.g., NbSe_2 , which is a low- T_c superconductor.^{26–28}

Figure 2(b) shows the V - I curves obtained at 70 K under various magnetic fields for the ZFC and FC modes for sample A. The V - I curves and the threshold current for the ZFC mode agree with those for the FC mode. This agreement implies that bulk pinning is weak because of strong thermal fluctuations at high temperatures. Consequently, the influence of crystal defects can be almost neglected at least above 70 K. In addition, the slope of the V - I curves changes prominently in the vicinity of 50 Oe. Below approximately 50 Oe, the V - I curves have a linear profile with a sudden appearance of voltage in a low-voltage region. On the other hand, above approximately 50 Oe, the V - I curves exhibit a nonlinear shape with a weak upturn, namely, flux creep due to thermal fluctuations appears in the low-voltage region. The change in the slope should reflect a change of the vortex state with the increase in the field. Moreover, even for magnetic fields below 50 Oe, the V - I curves have a drastic dependence on the field, though the slopes just after depinning are similar to each other.

J_c calculated from the V - I curves at 70–77 K is plotted as a function of the magnetic field in Fig. 3. At all the measured temperatures, J_c increases with the magnetic field below several tens of oersteds and reaches a peak. Further increases in the field lead to a reduction in J_c . The field at which the peak in J_c appears, H_{peak} , increases with decreasing temperature, as shown by the arrows in Fig. 3. This peak effect of J_c is different from the second-peak (SP) effect that is observed as a result of the order-disorder transition from the Bragg

glass^{29,30} to a disordered state of two-dimensional pancake vortices in Bi-2212 bulk single crystals without intensive bulk pinning.^{31–33} The following three aspects are brought to light by comparison with the SP effect. First, the SP effect in bulk single crystals normally emerges at temperatures below 40 K, whereas the peak effect in the whisker appears at high temperatures where thermal fluctuations dominate over the bulk pinning potential. Second, H_{peak} is dependent on the temperature and is shifted to higher fields with decreasing temperature, in contrast to the case of bulk single crystals, where the SP effect is independent of temperature or may have a weak temperature dependence owing to the inverse melting reported by Avraham *et al.* in Ref. 34. Finally, H_{peak} is much lower than that in the SP effect in bulk single crystals, which normally exhibit a peak in J_c under a magnetic field in the range of 200–1000 Oe on the basis of the three-to-two-dimensional crossover field varied by the strength of the superconducting anisotropy.³⁵ For example, H_{peak} of the data for 70 K in Fig. 3 is about 45 Oe. If the induction $B = 45$ G, the triangular vortex lattice constant is approximately $0.7 \mu\text{m}$. This suggests that H_{peak} is too low for the peak effect to be caused by chemical inhomogeneity. For dilute vortices in the low-field regime near H_{c1} , for example, when a magnetic field of 45 Oe is applied, the actual induction should be lower than 45 G. In this context, the vortex lattice constant will become larger than the value expected from the applied magnetic field.

Next, we evaluate H_{c1} and H_p at 70 K for the whisker. By assuming a coherence length³⁶ $\xi(0) = 2.3$ nm and penetration depth $\lambda(0) = 200$ nm,^{13,37} an H_{c1} value (at 70 K) of 53 Oe is obtained from the relation $H_{c1} \approx \Phi_0 \ln \kappa / 4\pi\lambda^2$, where Φ_0 is the quantum flux and κ is the Ginzburg-Landau (GL) parameter λ/ξ . On the basis of the study by Wang *et al.* on H_p in micrometer-sized Bi-2212 single crystals³⁸ and a high temperature of 70 K near T_c , the following formulas associated with the thickness-to-width ratio t/w are applied in the present work to estimate H_p in the two cases of BLSBs and GBs. As proposed by Burlachokov *et al.* for two-dimensional vortices,¹³ the penetration field governed by BLSBs is given by

$$H_{p,\text{BLSB}}(T) = \sqrt{\frac{t}{w}} H_c(T) \exp\left(-\frac{T}{T_0}\right), \quad (1)$$

where T_0 is the characteristic temperature with regard to the flux creep. On the other hand, the penetration field governed by GBs is given by

$$H_{p,\text{GB}}(T) = H_{c1}(T) \tanh \sqrt{0.36 \frac{t}{w}}, \quad (2)$$

which was proposed by Brandt for pin-free type-II superconductors.¹⁶ Consequently, a $H_{p,\text{BLSB}}(70 \text{ K})$ value of 29 Oe and a $H_{p,\text{GB}}(70 \text{ K})$ value of 11 Oe are obtained by using Eqs. (1) and (2), respectively. Here, T_0 of 25 K and the thermodynamic critical field $H_c(70 \text{ K})$ ($\approx \sqrt{2}\kappa H_{c1}/\ln \kappa$) are used for the calculation of $H_{p,\text{BLSB}}$.^{13,18} The estimated penetration fields are much lower than the calculated H_{c1} . In particular, $H_{p,\text{GB}}$ is compared to the value of approximately 13 Oe reported by Gregory *et al.* in Bi-2212 whiskers by

employing a local magnetization measurement.¹⁸ Therefore, the first vortex penetration to the center of the Bi-2212 whisker at high temperatures is possible by applying a magnetic field below H_{c1} because of the effect of surface barriers. As shown for the data of 70 K in Fig. 3, an enhancement of J_c is observed in the low-field regime above H_p and near the calculated H_{c1} . Moreover, the present peak effect is inconsistent with the peak effect observed at low temperatures by a global magnetization measurement in previous work;³⁹ the peak effect observed around 20 K in Bi-2212 whiskers reflects the first vortex penetration to the center of the sample owing to the asymmetric shape of the magnetization loop affected by surface barriers. In fact, the magnitude of H_{peak} estimated from the magnetization loop is similar to that of H_p reported by Gregory *et al.* in Ref. 18. However, for vortices penetrating to the center of the sample in the presence of magnetic fields below H_{c1} , the enhancement in J_c with the field is not due to the first vortex penetration, but due to the following reason.

With respect to dilute vortices that penetrate superconductors for $H < H_{c1}$, the vortex dome in the bulk single crystals should have a high orientation and a large correlation length for the vortex lattice; this was observed by Marchevsky *et al.* in NbSe₂ single crystals using the Bitter decoration technique.¹¹ However, in the case of dilute vortices in the Bi-2212 whiskers with small cross sections, the influence of the energy potential induced by surface barriers will reach the center of the sample owing to the narrow width; the distance from the center of the sample to the flux-free region near the surface is much shorter than that for bulk single crystals. In this context, the vortex distribution with an underdeveloped two-dimensional symmetry, for example, a one-dimensional-like vortex array along the a axis and weakly interacting (liquidlike) vortices confined to the whisker by surface barriers, should appear before the formation of the triangular vortex lattice. The change in the correlation of dilute vortices affects the field dependence of J_c . Therefore, the peak effect observed in the whisker is considered to be the result of the transition from the vortex state with the precursory configuration before the triangular vortex lattice formation to the quasicrystalline state of the two-dimensional vortex lattice, which is the Bragg glass (or may be the vortex crystal described by Beidenkopf *et al.* in a recent paper⁴⁰). In particular, when the sample dimension perpendicular to the magnetic field, i.e., the width of the whisker, is less than the order of the translational correlation length ($\sim 10a_0$, where a_0 is the intervortex spacing¹²) observed in bulk single crystals, the precursory state will be formed in a low-field regime before the emergence of the quasicrystalline state composed of the triangular vortex lattice. The interpretation with respect to the vortex distribution may be supported by the local magnetization of the Bi-2212 whiskers that was measured by James *et al.* at low fields.⁴¹ Sharp jumps in the local magnetic induction also suggest a change in the configuration of vortices confined to the strip geometry by the surface barriers.

On the other hand, in the absence of the size effect, the peak effect in the low-field regime does not emerge for $H > H_p$, as described by Elistratov *et al.* for an edge-dominant condition similar to the present situation.⁴² Moreover, ac-

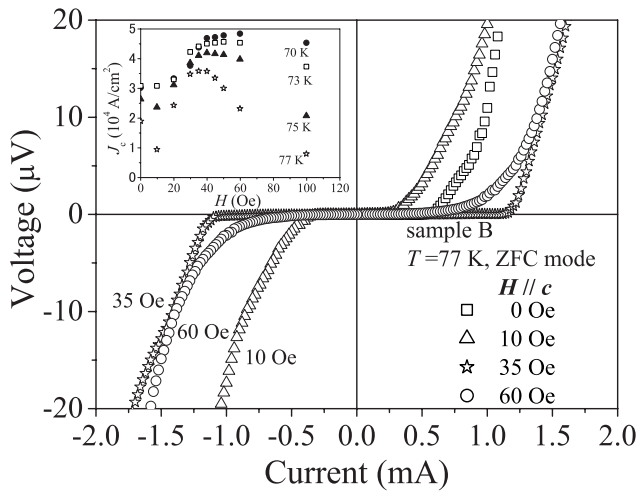


FIG. 4. V - I characteristics with the configuration of $I \parallel a$ axis and $H \parallel c$ axis at 77 K for the ZFC mode for sample B. The inset shows the field dependence of J_c estimated from the V - I curves at temperatures in the range 70–77 K. H_{peak} varies from 35 to 60 Oe as the temperature is reduced from 77 to 70 K.

According to the collective pinning model proposed by Larkin and Ovchinnikov,⁴³ J_c for $H > H_p$ should be inversely proportional to the field if the correlation volume is almost independent of the field in the low-field regime. The behavior in the absence of the size effect is obviously different from the present results in which the peak effect is observed.

In the inset of Fig. 3, critical current densities normalized by the maximum value of J_c , i.e., the magnitude of $J_c(H_{\text{peak}})$, are plotted as a function of the magnetic field normalized by the magnitude of H_{peak} . For $H/H_{\text{peak}} < 1$, the reduced critical current densities are almost independent of temperature, whereas for $H/H_{\text{peak}} > 1$, they are inversely dependent on the temperature. This indicates that the manner of dissipation due to vortex motion is changed at H_{peak} . For high magnetic fields ($>H_{\text{peak}}$) where the vortices are in the quasiordered state, thermal fluctuations apparently contributed to the vortex depinning; this means that vortices overcome the energy potential induced by surface barriers and move in a direction assisted by the driving force due to transport currents. On the other hand, for low magnetic fields ($<H_{\text{peak}}$ and H_{c1}), vortices that enter the sample owing to thermal fluctuations participate in the vortex state with underdeveloped two-dimensional symmetry and almost do not exit from the sample because the vortices are pushed toward the center of the sample by the Lorentz force due to the Meissner current when the transport current is low. Consequently, the thermal contribution to vortex depinning is weak, namely, the flux creep due to thermal fluctuations is suppressed in the vortex state with the precursory configuration before triangular vortex lattice formation. The vortex dynamics that contributed to the dissipation for $H < H_{\text{peak}}$ will be mainly due to the driving force induced by a high transport current. Further support for the interpretation comes from the result that the V - I curves in the low-voltage region for $H < H_{\text{peak}}$ exhibit an almost linear slope similar to the behavior observed at low temperatures. For high fields ($H > H_{\text{peak}}$), the influence of the flux creep due to thermal fluctuations of the quasiordered

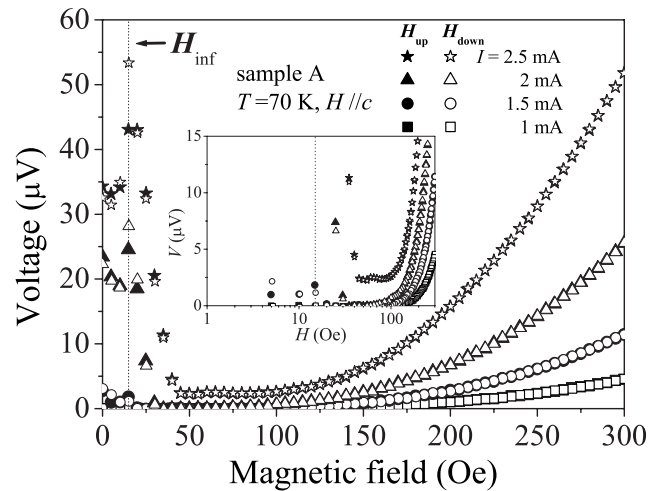


FIG. 5. Field dependence of the voltage at 70 K on sample A for fixed transport currents ($\parallel a$ axis) above and below the critical current obtained under the self-field. The closed and open symbols represent the ascending and descending branches of the field, respectively. The low-voltage region is enlarged in the inset, where a logarithmic H scale is used for convenience in displaying the data.

vortex state obviously appears in the V - I characteristics [see Figs. 2(a) and 2(b)].

Figure 4 shows the V - I curves obtained under magnetic fields at 77 K for the ZFC mode for sample B (in the main panel) and the field dependence of J_c obtained at temperatures of 70–77 K (in the inset). An enhancement in J_c is observed in the presence of low magnetic fields at all the measured temperatures (70, 73, 75, and 77 K) for sample B as well as sample A, as shown in the inset of Fig. 4. H_{peak} is slightly higher than that at a given temperature for sample A. For example, for the data of 70 K, sample A with a width of $7.1\ \mu\text{m}$ and sample B with a width of $5.4\ \mu\text{m}$ exhibit H_{peak} values of 45 and 60 Oe, respectively. The difference between samples A and B with regard to the magnitude of H_{peak} is consistent with the scenario of the peak effect attributed to the sample size; the smaller the width of a sample, the higher the magnetic field required for vortices to form a triangular vortex lattice. Note that the peak effect occurs independent of the reverse transport current. In Fig. 4, the threshold current of the V - I curve for 10 Oe is lower than that for 35 Oe irrespective of the sign of the transport current. Therefore, the peak effect does not result from the effect of asymmetric surface barriers described by Vodolazov and Peeters in Ref. 44.

The peak effect in the Bi-2212 whiskers is confirmed not only by the behavior of the V - I curves, but also by a field-induced zero-voltage state detected with a step-by-step magnetic field ramping, as shown in Fig. 5; here, the voltage V is plotted as a function of the magnetic field H . A low-field region is enlarged in the inset. The data for sample A were obtained at a constant temperature of 70 K and for a fixed transport current, with several values in the range 1.0–2.5 mA. The V - H profile for the low transport current of 1.0 mA (approximately $1.8 \times 10^4\text{ A/cm}^2$) exhibits the simple features observed normally in Bi-2212 bulk samples,⁴⁵ the voltage appears above a threshold field, and then gradually

increases with the field. The profile for the higher transport currents (1.5 and 2.0 mA) has the following field-induced zero-voltage state in the low-field regime. For example, in the profile for 2.0 mA (approximately 3.5×10^4 A/cm²), a voltage appears in the absence of a magnetic field and in the presence of low magnetic fields; subsequently, it rapidly disappears above an influential field H_{inf} . Further increases in the field lead to the reappearance of the voltage. In the profile for 2.5 mA (approximately 4.4×10^4 A/cm²), the Lorentz force due to the high transport current accelerates the vortex depinning. Consequently, the field-induced zero-voltage state vanishes and a finite-voltage state appears in the entire region of the fields. H_{inf} is approximately 15 Oe under the present conditions. For magnetic fields above H_{inf} , the field-ascending branch agrees with the field-descending branch. The reversibility suggests that the peak effect shown in Fig. 3 has no relation not only to the generation of a metastable vortex state due to edge contaminations, but also to the heating due to the Joule effect that takes place at the electrical contacts. According to the experiment by Nideröst *et al.*,⁴⁶ the penetration of the magnetic flux is dependent on the ramping rate of the field. In the present work, the ramping time to the individual target fields is approximately 60 s. Moreover, the transport current density is higher than 1.8×10^4 A/cm², which is estimated on the basis of the assumption of homogeneous current flow. Therefore, the BLSBs should be ineffective in the suppression of the flux penetration because of the slow rate of the ramping field, the thermal fluctuations due to the high temperatures, and the driving force due to the transport current. This is supported by the result that the magnitude of H_{inf} is close to that of H_p estimated for the GBs. Although interpreting H_{inf} in practice is difficult because of the dynamic measurement in the present experiment, the remarkable reduction in the voltage above H_{inf} appears to be associated with the crossover in the vortex state from weakly interacting vortices (like single vortices) to a bundle due to an enhanced interaction between vortices just before the formation of the triangular vortex lattice. Here, the current density levels corresponding to transport currents 1.0 and 2.0 mA are shown by the dotted and dashed lines in Fig. 3, respectively. The V - H curves for 1.0 and 2.0 mA express the feature of the $J_c(H)$ profile shown in Fig. 3 well: a finite-voltage state above the $J_c(H)$ curve and a zero-voltage state below. The field-induced zero-voltage state is also observed at the other measured temperatures (73, 75, and 77 K) for high transport currents above the critical current obtained under a self-induced magnetic field. Moreover, sample B also exhibits such a field-induced zero-voltage state.

An enhancement in J_c with the magnetic field H at temperatures T near T_c has been reported in untwinned overdoped YBa₂Cu₃O₇ (YBCO) single crystals^{47,48} and NbSe₂ single crystals.⁴⁹ However, the magnetic field at which a peak in $J_c(H)$ appears is much higher than H_{peak} in the Bi-2212 whiskers; the H_{peak} in YBCO and NbSe₂ are in the range of a few kilo-oersteds to several tens of kilo-oersteds. Although the exact origin for the peak effects of the two superconducting materials may be controversial, schematic scenarios for the occurrence of the peak effects are as follows. As described theoretically by Ikeda in Ref. 50, in the

case of the YBCO system, the lower critical point H_{lcp} is enhanced owing to the small anisotropy in contrast to Bi-2212 superconductors. The peak effect near T_c emerges as the signature of an order-disorder transition because vortex-lattice melting and irreversibility lines are different from each other with regard to the temperature dependence at high temperatures above H_{lcp} .⁴⁷ Normally, H_{lcp} in Bi-2212 single crystals cannot be observed owing to the high anisotropy; therefore, the peak effect for fields below H_{lcp} will be undetectable in the Bi-2212 material. On the other hand, in the case of the NbSe₂ system, the peak effect near T_c is observed as an order-disorder transition from the Bragg glass to a disordered phase such as a polycrystalline solid in the magnetic field region close to the upper critical field H_{c2} when the magnetic field or temperature is varied in the temperature region near T_c in the H - T plane.^{51,52} Therefore, the individual scenarios of these peak effects appear to be different from that of the present peak effect observed in the low-field regime near the calculated H_{c1} in the Bi-2212 whiskers.

For Bi-2212 bulk single crystals with a strong disorder and/or a reduced anisotropy, the vortex-lattice melting (H_m) line is pushed slightly downward in the H - T plane owing to the effect of bulk pinning;⁵³ therefore, the SP effect is observable up to the vicinity of T_c .^{32,54,55} Contrary to the present peak effect, the SP effect is a result of the order-disorder transition from a long-range-ordered vortex state to a disordered vortex state due to bulk pinning, and the H_{peak} line at high temperatures in the H - T plane lies close to the H_m line rather than the H_{c1} line. The present peak effect seems to bear little relation to the SP effect.

The reproducible results of the present work indicate that the peak effect of J_c at high temperatures and the resulting concave voltage response to the fields are not artificial effects but intrinsic phenomena attributed to the surface barriers and the narrow widths of the Bi-2212 whiskers. In particular, the nonlinear response of the concave V - H curves should accelerate the application of the Bi-system high- T_c superconducting whiskers to electronic devices because the phenomenon occurs under low magnetic fields below several hundred oersteds.

IV. CONCLUSION

We have investigated the V - I characteristics with the configuration of $I \parallel a$ axis and $H \parallel c$ axis in Bi-2212 whiskers. At high temperatures above 70 K, J_c increases and exhibits a peak below several tens of oersteds before decreasing monotonically with the increasing field. Contrary to the case of Bi-2212 bulk single crystals, the peak effect occurs in the low-field regime near H_{c1} . The field at which a peak of $J_c(H)$ appears is dependent on temperature. In addition, the peak effect is consistent with a field-induced zero voltage that is measured at a constant temperature and fixed transport current with a step-by-step field ramping. The enhancement in J_c with the field is related to dilute vortices, which enter the samples owing to the effect of surface barriers. This phenomenon suggests a transition from a vortex state with a precursory vortex configuration induced by the narrow widths of the whiskers to a quasiordered state composed of the triangular vortex lattice.

ACKNOWLEDGMENTS

We would like to thank T. Koyano of Cryogenics Division, The University of Tsukuba, for engaging in helpful dis-

cussions. We also would like to acknowledge T. Tamegai of the University of Tokyo for useful discussions and S. Kasahara for experimental advice. M.T. is grateful to the JSPS for financial support.

- ¹C. P. Bean and J. D. Livingston, Phys. Rev. Lett. **12**, 14 (1964).
- ²M. V. Indenbom, G. D'Anna, M.-O. André, V. V. Kabanov, and W. Benoit, Physica C **235–240**, 201 (1994).
- ³E. Zeldov, A. I. Larkin, V. B. Geshkenbein, M. Konczykowski, D. Majer, B. Khaykovich, V. M. Vinokur, and H. Shtrikman, Phys. Rev. Lett. **73**, 1428 (1994).
- ⁴C. P. Bean, Phys. Rev. Lett. **8**, 250 (1962).
- ⁵D. T. Fuchs, R. A. Doyle, E. Zeldov, S. F. W. R. Rycroft, T. Tamegai, S. Ooi, M. L. Rappaport, and Y. Myasoedov, Phys. Rev. Lett. **81**, 3944 (1998).
- ⁶N. Chikumoto, M. Konczykowski, N. Motohira, and A. P. Malozemoff, Phys. Rev. Lett. **69**, 1260 (1992).
- ⁷L. Burlachkov, Phys. Rev. B **47**, 8056 (1993); L. Burlachkov, A. E. Koshelev, and V. M. Vinokur, *ibid.* **54**, 6750 (1996).
- ⁸M. V. Indenbom, H. Kronmüller, T. W. Li, P. H. Kes, and A. A. Menovsky, Physica C **222**, 203 (1994).
- ⁹Th. Schuster, M. V. Indenbom, H. Kuhn, E. H. Brandt, and M. Konczykowski, Phys. Rev. Lett. **73**, 1424 (1994).
- ¹⁰M. W. Gardner, S. A. Govorkov, R. Liang, D. A. Bonn, J. F. Carolan, and W. N. Hardy, J. Appl. Phys. **83**, 3714 (1998).
- ¹¹M. Marchevsky, L. A. Gurevich, P. H. Kes, and J. Aarts, Phys. Rev. Lett. **75**, 2400 (1995).
- ¹²C. A. Murray, P. L. Gammel, D. J. Bishop, D. B. Mitzi, and A. Kapitulnik, Phys. Rev. Lett. **64**, 2312 (1990).
- ¹³L. Burlachkov, V. B. Geshkenbein, A. E. Koshelev, A. I. Larkin, and V. M. Vinokur, Phys. Rev. B **50**, 16770 (1994).
- ¹⁴M. Benkraouda and J. R. Clem, Phys. Rev. B **53**, 5716 (1996).
- ¹⁵A. V. Kuznetsov, D. V. Eremanko, and V. N. Trofimov, Phys. Rev. B **56**, 9064 (1997).
- ¹⁶E. H. Brandt, Phys. Rev. B **60**, 11939 (1999).
- ¹⁷M. S. James, S. T. Stoddart, S. J. Bending, S. Aukkaravittayapun, P. J. King, and M. Henini, Phys. Rev. B **56**, R5771 (1997).
- ¹⁸J. K. Gregory, M. S. James, S. J. Bending, C. J. van der Beek, and M. Konczykowski, Phys. Rev. B **64**, 134517 (2001).
- ¹⁹N. Morozov, E. Zeldov, M. Konczykowski, and R. A. Doyle, Physica C **291**, 113 (1997).
- ²⁰D. Majer, E. Zeldov, and M. Konczykowski, Phys. Rev. Lett. **75**, 1166 (1995).
- ²¹R. A. Doyle, S. F. W. R. Rycroft, C. D. Dewhurst, E. Zeldov, I. Tsabba, S. Reich, T. B. Doyle, T. Tamegai, and S. Ooi, Physica C **308**, 123 (1998).
- ²²M. Tange, T. Amano, S. Nishizaki, and R. Yoshizaki, Physica C **392–396**, 428 (2003).
- ²³When annealing of the as-grown Bi-2212 whiskers synthesized under the same growth condition takes place at 600 °C under an oxygen partial pressure of 0.01 atm to remove the excess oxygen, T_c rises to approximately 83.5 K. Therefore, the presented whiskers are estimated to be slightly overdoped. The estimation is valid considering the suppression of maximum T_c , which was reported on the basis of the Bi-substitution level of $\text{Bi}_{2+x}\text{Sr}_{2-x}\text{CaCu}_2\text{O}_{8+\delta}$ single crystals [H. Eisaki, N. Kaneko, D. L. Feng, A. Damascelli, P. K. Mang, K. M. Shen, Z.-X. Shen, and M. Greven, Phys. Rev. B **69**, 064512 (2004)], as well as the relation of the excess oxygen to the annealing conditions for Bi-2212 single crystals [T. Watanabe, T. Fujii, and A. Matsuda, Phys. Rev. Lett. **79**, 2113 (1997)].
- ²⁴Y. Paltiel *et al.*, Phys. Rev. Lett. **85**, 3712 (2000).
- ²⁵Y. Paltiel, E. Zeldov, Y. N. Myasoedov, H. Shtrikman, S. Bhattacharya, M. J. Higgins, Z. L. Xiao, E. Y. Andrei, P. L. Gammel, and D. J. Bishop, Nature (London) **403**, 398 (2000).
- ²⁶W. Henderson, E. Y. Andrei, M. J. Higgins, and S. Bhattacharya, Phys. Rev. Lett. **77**, 2077 (1996).
- ²⁷Z. L. Xiao, E. Y. Andrei, P. Shuk, and M. Greenblatt, Phys. Rev. Lett. **85**, 3265 (2000).
- ²⁸Z. L. Xiao, E. Y. Andrei, P. Shuk, and M. Greenblatt, Phys. Rev. Lett. **86**, 2431 (2001).
- ²⁹T. Giamarchi and P. Le Doussal, Phys. Rev. B **52**, 1242 (1995).
- ³⁰T. Nattermann and S. Scheidl, Adv. Phys. **49**, 607 (2000).
- ³¹B. Khaykovich, E. Zeldov, D. Majer, T. W. Li, P. H. Kes, and M. Konczykowski, Phys. Rev. Lett. **76**, 2555 (1996).
- ³²S. Ooi, T. Tamegai, and T. Shibauchi, J. Low Temp. Phys. **105**, 1011 (1996).
- ³³M. B. Gaifullin, Y. Matsuda, N. Chikumoto, J. Shimoyama, and K. Kishio, Phys. Rev. Lett. **84**, 2945 (2000).
- ³⁴N. Avraham *et al.*, Nature (London) **411**, 451 (2001).
- ³⁵V. M. Vinokur, P. H. Kes, and A. E. Koshelev, Physica C **168**, 29 (1990).
- ³⁶Y. Wang, S. Ono, Y. Onose, G. Gu, Y. Ando, Y. Tokura, S. Uchida, and N. P. Ong, Science **299**, 86 (2003).
- ³⁷S. L. Lee *et al.*, Phys. Rev. Lett. **71**, 3862 (1993).
- ³⁸Y. M. Wang, A. Zettl, S. Ooi, and T. Tamegai, Phys. Rev. B **65**, 184506 (2002).
- ³⁹M. Tange, T. Amano, S. Nishizaki, and R. Yoshizaki, Physica C **408–410**, 872 (2004).
- ⁴⁰H. Beidenkopf, N. Avraham, Y. Myasoedov, H. Shtrikman, E. Zeldov, B. Rosenstein, E. H. Brandt, and T. Tamegai, Phys. Rev. Lett. **95**, 257004 (2005).
- ⁴¹M. S. James, S. J. Bending, S. T. Stoddart, S. Aukkaravittayapun, P. J. King, and M. Henini, IEEE Trans. Appl. Supercond. **9**, 2671 (1999).
- ⁴²A. A. Elistratov, D. Yu. Vodolozov, I. L. Maksimov, and J. R. Clem, Phys. Rev. B **66**, 220506(R) (2002).
- ⁴³A. I. Larkin and Yu. N. Ovchinnikov, J. Low Temp. Phys. **34**, 409 (1979).
- ⁴⁴D. Y. Vodolozov and F. M. Peeters, Phys. Rev. B **72**, 172508 (2005).
- ⁴⁵D. T. Fuchs, E. Zeldov, D. Majer, R. A. Doyle, T. Tamegai, S. Ooi, and M. Konczykowski, Phys. Rev. B **54**, R796 (1996).
- ⁴⁶M. Nideröst, R. Frassanito, M. Saalfrank, A. C. Mota, G. Blatter, V. N. Zavaritsky, T. W. Li, and P. H. Kes, Phys. Rev. Lett. **81**, 3231 (1998).
- ⁴⁷T. Nishizaki, K. Shibata, T. Sasaki, and N. Kobayashi, Physica C

- 341–348**, 957 (2000).
- ⁴⁸A. A. Zhukov *et al.*, Phys. Rev. Lett. **87**, 017006 (2001).
- ⁴⁹S. Bhattacharya and M. J. Higgins, Phys. Rev. Lett. **70**, 2617 (1993).
- ⁵⁰R. Ikeda, J. Phys. Soc. Jpn. **70**, 219 (2001).
- ⁵¹M. Menghini, Y. Fasano, and F. de la Cruz, Phys. Rev. B **65**, 064510 (2002).
- ⁵²Y. Fasano, M. Menghini, F. de la Cruz, Y. Paltiel, Y. Myasoedov, E. Zeldov, M. J. Higgins, and S. Bhattacharya, Phys. Rev. B **66**, 020512(R) (2002).
- ⁵³G. P. Mikitik and E. H. Brandt, Phys. Rev. B **68**, 054509 (2003).
- ⁵⁴M. Baziljevich, D. Giller, M. McElfresh, Y. Abulafia, Y. Radzyner, J. Schneck, T. H. Johansen, and Y. Yeshurun, Phys. Rev. B **62**, 4058 (2000).
- ⁵⁵K. K. Uprety, J. Horvat, X. L. Wang, M. Ionescu, H. K. Liu, S. X. Dou, and E. H. Brandt, Phys. Rev. B **65**, 224501 (2002).